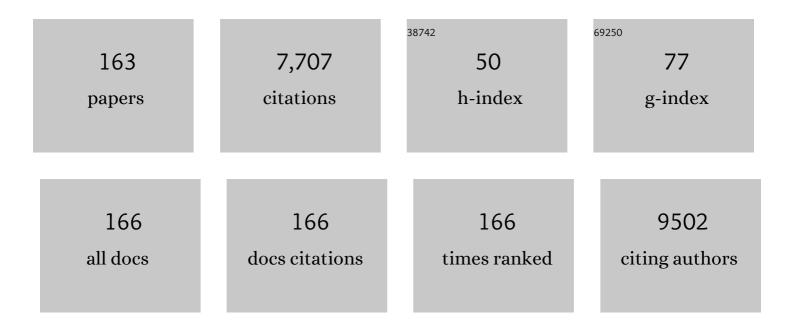
## Mingbo Wu

List of Publications by Year in descending order

Source: https://exaly.com/author-pdf/7204337/publications.pdf Version: 2024-02-01



MINGRO WU

#	Article	IF	CITATIONS
1	Intrinsic Mechanisms of Morphological Engineering and Carbon Doping for Improved Photocatalysis of 2D/2D Carbon Nitride Van Der Waals Heterojunction. Energy and Environmental Materials, 2023, 6, .	12.8	17
2	The Nature of Active Sites for Plasmonâ€Mediated Photothermal Catalysis and Heatâ€Coupled Photocatalysis in Dry Reforming of Methane. Energy and Environmental Materials, 2023, 6, .	12.8	4
3	Polycyclic Aromatic Hydrocarbons as a New Class of Promising Cathode Materials for Aluminumâ€lon Batteries. Angewandte Chemie - International Edition, 2022, 61, e202114681.	13.8	37
4	Polycyclic Aromatic Hydrocarbons as a New Class of Promising Cathode Materials for Aluminumâ€lon Batteries. Angewandte Chemie, 2022, 134, .	2.0	7
5	Ammonia etched petroleum pitch-based porous carbon as efficient catalysts for CO2 electroreduction. Carbon Letters, 2022, 32, 807-814.	5.9	5
6	A "Trojan horse―strategy towards robust Co–N <sub>4</sub> active sites accommodated in micropore defect-rich carbon nanosheets for boosting selective hydrogenation of nitroarenes. Journal of Materials Chemistry A, 2022, 10, 9435-9444.	10.3	12
7	In Situ-Fabricated In <sub>2</sub> S <sub>3</sub> -Reduced Graphene Oxide Nanosheet Composites for Enhanced CO <sub>2</sub> Electroreduction to Formate. ACS Applied Nano Materials, 2022, 5, 2335-2342.	5.0	13
8	Kinetically accelerated and high-mass loaded lithium storage enabled by atomic iron embedded carbon nanofibers. Nano Research, 2022, 15, 6176-6183.	10.4	12
9	Regulation of energetic hot carriers on Pt/TiO2 with thermal energy for photothermal catalysis. Applied Catalysis B: Environmental, 2022, 309, 121263.	20.2	38
10	Oxygenâ€Deficient Metal Oxides for Supercapacitive Energy Storage: From Theoretical Calculation to Structural Regulation and Utilization. Advanced Energy and Sustainability Research, 2022, 3, .	5.8	5
11	A metal–organic framework-modified separator enables long cycling lithium-ion capacitors with asymmetric electrolyte design. Journal of Materials Chemistry A, 2022, 10, 19852-19858.	10.3	8
12	Trace nitrogen-incorporation stimulates dual active sites of nickel catalysts for efficient hydrogen oxidation electrocatalysis. Chemical Engineering Journal, 2022, 445, 136700.	12.7	11
13	Engineering controllable oxygen vacancy defects in iron hydroxide oxide immobilized on reduced graphene oxide for boosting visible light-driven photo-Fenton-like oxidation. Journal of Colloid and Interface Science, 2022, 623, 9-20.	9.4	22
14	Petroleum pitch derived carbon as both cathode and anode materials for advanced potassium-ion hybrid capacitors. Carbon, 2022, 196, 727-735.	10.3	17
15	Cu <sub>3</sub> N nanoparticles with both (100) and (111) facets for enhancing the selectivity and activity of CO <sub>2</sub> electroreduction to ethylene. New Journal of Chemistry, 2022, 46, 12523-12529.	2.8	5
16	<scp>CoN</scp> graphene encapsulated cobalt catalyst for <scp>H<sub>2</sub>O<sub>2</sub></scp> decomposition under acidic conditions. AICHE Journal, 2022, 68, .	3.6	3
17	Dual carbon Li-ion capacitor with high energy density and ultralong cycling life at a wide voltage window. Science China Materials, 2022, 65, 2373-2384.	6.3	5
18	Localized Surface Plasmon Resonance Enhanced Continuous Flow Photoelectrocatalytic CO <sub>2</sub> Conversion to CO. Energy & Fuels, 2022, 36, 7206-7212.	5.1	10

#	Article	IF	CITATIONS
19	Petroleum pitch-derived porous carbon as a metal-free catalyst for direct propane dehydrogenation to propylene. Catalysis Today, 2022, , .	4.4	2
20	Efficient CO2 electroreduction over N-doped hieratically porous carbon derived from petroleum pitch. Journal of Energy Chemistry, 2021, 56, 113-120.	12.9	21
21	High-performance aluminum-polyaniline battery based on the interaction between aluminum ion and -NH groups. Science China Materials, 2021, 64, 318-328.	6.3	31
22	Non-corrosive and low-cost synthesis of hierarchically porous carbon frameworks for high-performance lithium-ion capacitors. Carbon, 2021, 173, 646-654.	10.3	40
23	Reinforced atomically dispersed Fe N C catalysts derived from petroleum asphalt for oxygen reduction reaction. Journal of Colloid and Interface Science, 2021, 587, 810-819.	9.4	23
24	PVP-assisted synthesis of ultrafine transition metal oxides encapsulated in nitrogen-doped carbon nanofibers as robust and flexible anodes for sodium-ion batteries. Carbon, 2021, 174, 325-334.	10.3	31
25	Thermal Driven High Crystallinity of Bismuth as Robust Catalyst for CO <sub>2</sub> Electroreduction to Formate. ChemistrySelect, 2021, 6, 1870-1873.	1.5	2
26	Boosting the Pseudocapacitive and High Mass‣oaded Lithium/Sodium Storage through Bonding Polyoxometalate Nanoparticles on MXene Nanosheets. Advanced Functional Materials, 2021, 31, 2007636.	14.9	53
27	Innentitelbild: Fe/Fe <sub>3</sub> C Boosts H <sub>2</sub> O <sub>2</sub> Utilization for Methane Conversion Overwhelming O <sub>2</sub> Generation (Angew. Chem. 16/2021). Angewandte Chemie, 2021, 133, 8642-8642.	2.0	0
28	Fe/Fe <sub>3</sub> C Boosts H <sub>2</sub> O <sub>2</sub> Utilization for Methane Conversion Overwhelming O <sub>2</sub> Generation. Angewandte Chemie, 2021, 133, 8971-8977.	2.0	26
29	Threeâ€dimensional printing of highâ€mass loading electrodes for energy storage applications. InformaÄnÃ- Materiály, 2021, 3, 631-647.	17.3	50
30	Fe/Fe <sub>3</sub> C Boosts H <sub>2</sub> O <sub>2</sub> Utilization for Methane Conversion Overwhelming O <sub>2</sub> Generation. Angewandte Chemie - International Edition, 2021, 60, 8889-8895.	13.8	66
31	Cu,Zn Dopants Boost Electron Transfer of Carbon Dots for Antioxidation. Small, 2021, 17, e2102178.	10.0	40
32	Precious potential regulation of carbon cathode enabling high-performance lithium-ion capacitors. Carbon, 2021, 180, 110-117.	10.3	19
33	Cu,Zn Dopants Boost Electron Transfer of Carbon Dots for Antioxidation (Small 31/2021). Small, 2021, 17, 2170162.	10.0	0
34	Unraveling the Synergy of Chemical Hydroxylation and the Physical Heterointerface upon Improving the Hydrogen Evolution Kinetics. ACS Nano, 2021, 15, 15017-15026.	14.6	59
35	Photocatalytic Câ^'F Bond Activation of Fluoroarenes, <i>gem</i> â€Difluoroalkenes and Trifluoromethylarenes. Asian Journal of Organic Chemistry, 2021, 10, 2454-2472.	2.7	32
36	Direct Conversion of CO <sub>2</sub> to Ethanol Boosted by Intimacy-Sensitive Multifunctional Catalysts. ACS Catalysis, 2021, 11, 11742-11753.	11.2	69

#	Article	IF	CITATIONS
37	Carbon dots-oriented synthesis of fungus-like CoP microspheres as a bifunctional electrocatalyst for efficient overall water splitting. Carbon, 2021, 182, 327-334.	10.3	46
38	Robust and Fast Lithium Storage Enabled by Polypyrrole-Coated Nitrogen and Phosphorus Co-Doped Hollow Carbon Nanospheres for Lithium-Ion Capacitors. Frontiers in Chemistry, 2021, 9, 760473.	3.6	8
39	Single-Atom Fe-N4 sites promote the triplet-energy transfer process of g-C3N4 for the photooxidation. Journal of Catalysis, 2021, 404, 89-95.	6.2	26
40	Porous g-C3N4 and α-FeOOH bridged by carbon dots as synergetic visible-light-driven photo-fenton catalysts for contaminated water remediation. Carbon, 2021, 183, 628-640.	10.3	46
41	Aligning potential differences within carbon nitride based photocatalysis for efficient solar energy harvesting. Nano Energy, 2021, 89, 106357.	16.0	41
42	Carbon sustained SnO2-Bi2O3 hollow nanofibers as Janus catalyst for high-efficiency CO2 electroreduction. Chemical Engineering Journal, 2021, 426, 131867.	12.7	24
43	Thermocatalytic hydrogenation of <scp>CO<sub>2</sub></scp> into aromatics by tailorâ€made catalysts: Recent advancements and perspectives. EcoMat, 2021, 3, e12080.	11.9	29
44	Boosting the synthesis of value-added aromatics directly from syngas <i>via</i> a Cr <sub>2</sub> O <sub>3</sub> and Ga doped zeolite capsule catalyst. Chemical Science, 2021, 12, 7786-7792.	7.4	18
45	Flexible electrodes with high areal capacity based on electrospun fiber mats. Nanoscale, 2021, 13, 18391-18409.	5.6	15
46	Iron-Catalyzed Remote C–H Alkylation of 8-Amidoquinolines with Cycloalkanes. Synthesis, 2021, 53, 3144-3150.	2.3	3
47	In Situ Construction of Nickel Sulfide Nano-Heterostructures for Highly Efficient Overall Urea Electrolysis. ACS Sustainable Chemistry and Engineering, 2021, 9, 15582-15590.	6.7	17
48	Hierarchically micro- and meso-porous Fe-N4O-doped carbon as robust electrocatalyst for CO2 reduction. Applied Catalysis B: Environmental, 2020, 266, 118630.	20.2	74
49	Template-Oriented Synthesis of Fe–N-Codoped Graphene Nanoshells Derived from Petroleum Pitch for Efficient Nitroaromatics Reduction. Industrial & Engineering Chemistry Research, 2020, 59, 129-136.	3.7	17
50	Small graphite nanoflakes as an advanced cathode material for aluminum ion batteries. Chemical Communications, 2020, 56, 1593-1596.	4.1	24
51	The Crystallinity of Metal Oxide in Carbonized Metal Organic Frameworks and the Effect on Restricting Polysulfides. ChemNanoMat, 2020, 6, 274-279.	2.8	8
52	Alkali Halide Boost of Carbon Nitride for Photocatalytic H <sub>2</sub> Evolution in Seawater. ACS Applied Materials & Interfaces, 2020, 12, 48526-48532.	8.0	19
53	A Hydrogen-Initiated Chemical Epitaxial Growth Strategy for In-Plane Heterostructured Photocatalyst. ACS Nano, 2020, 14, 17505-17514.	14.6	41
54	Controllable Substitution of S Radicals on Triazine Covalent Framework to Expedite Degradation of Polysulfides. Small, 2020, 16, e2004631.	10.0	19

#	Article	IF	CITATIONS
55	Sub-5-nm Monolayer Silicane Transistor: A First-Principles Quantum Transport Simulation. Physical Review Applied, 2020, 14, .	3.8	38
56	Regulation of the cathode for amphi-charge storage in a redox electrolyte for high-energy lithium-ion capacitors. Chemical Communications, 2020, 56, 12777-12780.	4.1	9
57	Ohmic contacts of monolayer Tl2O field-effect transistors. Journal of Materials Science, 2020, 55, 11439-11450.	3.7	9
58	Heavy oil-derived carbon for energy storage applications. Journal of Materials Chemistry A, 2020, 8, 7066-7082.	10.3	57
59	Controllable Synthesis of Leaf‣ike CuO Nanosheets for Selective CO <sub>2</sub> Electroreduction to Ethylene. ChemElectroChem, 2020, 7, 2020-2025.	3.4	38
60	Laser Irradiation of Electrode Materials for Energy Storage and Conversion. Matter, 2020, 3, 95-126.	10.0	74
61	Intrinsic Defect-Rich Hierarchically Porous Carbon Architectures Enabling Enhanced Capture and Catalytic Conversion of Polysulfides. ACS Nano, 2020, 14, 6222-6231.	14.6	89
62	Facile and cost-effective manipulation of hierarchical carbon nanosheets for pseudocapacitive lithium/potassium storage. Carbon, 2020, 165, 296-305.	10.3	29
63	Controllably Enriched Oxygen Vacancies through Polymer Assistance in Titanium Pyrophosphate as a Super Anode for Na/K-Ion Batteries. ACS Nano, 2019, 13, 9227-9236.	14.6	94
64	Manipulation of interlayer spacing and surface charge of carbon nanosheets for robust lithium/sodium storage. Carbon, 2019, 153, 372-380.	10.3	39
65	Reexamination of the Schottky Barrier Heights in Monolayer MoS <sub>2</sub> Field-Effect Transistors. ACS Applied Nano Materials, 2019, 2, 4717-4726.	5.0	27
66	Amorphous Al <sub>2</sub> O <sub>3</sub> with N-Doped Porous Carbon as Efficient Polysulfide Barrier in Li–S Batteries. ACS Applied Energy Materials, 2019, 2, 1266-1273.	5.1	47
67	Cubic Cu2O on nitrogen-doped carbon shells for electrocatalytic CO2 reduction to C2H4. Carbon, 2019, 146, 218-223.	10.3	56
68	Extended lattice space of TiO2 hollow nanocubes for improved sodium storage. Chemical Engineering Journal, 2019, 373, 565-571.	12.7	25
69	Green and scalable synthesis of porous carbon nanosheet-assembled hierarchical architectures for robust capacitive energy harvesting. Carbon, 2019, 152, 537-544.	10.3	45
70	Chemical state of surrounding iron species affects the activity of Fe-Nx for electrocatalytic oxygen reduction. Applied Catalysis B: Environmental, 2019, 251, 240-246.	20.2	101
71	Interface-induced controllable synthesis of Cu2O nanocubes for electroreduction CO2 to C2H4. Electrochimica Acta, 2019, 306, 360-365.	5.2	35
72	Further activation of g-C3N4 with less N-H defects for enhancing photocatalytic hydrogen evolution. Catalysis Communications, 2019, 125, 114-117.	3.3	2

#	Article	IF	CITATIONS
73	Synthesis of Biomass-Derived Nitrogen-Doped Porous Carbon Nanosheests for High-Performance Supercapacitors. ACS Sustainable Chemistry and Engineering, 2019, 7, 8405-8412.	6.7	203
74	Graphene oxide-induced synthesis of button-shaped amorphous Fe2O3/rGO/CNFs films as flexible anode for high-performance lithium-ion batteries. Chemical Engineering Journal, 2019, 369, 215-222.	12.7	79
75	Physical vapor deposition (PVD): a method to fabricate modified g-C3N4 sheets. New Journal of Chemistry, 2019, 43, 6683-6687.	2.8	14
76	Robust NiCoP/CoP Heterostructures for Highly Efficient Hydrogen Evolution Electrocatalysis in Alkaline Solution. ACS Applied Materials & amp; Interfaces, 2019, 11, 15528-15536.	8.0	139
77	Schottky Contact in Monolayer WS <sub>2</sub> Fieldâ€Effect Transistors. Advanced Theory and Simulations, 2019, 2, 1900001.	2.8	42
78	Pyridinic Nitrogenâ€Doped Graphene Nanoshells Boost the Catalytic Efficiency of Palladium Nanoparticles for the <i>N</i> â€Allylation Reaction. ChemSusChem, 2019, 12, 858-865.	6.8	18
79	N-doped reduced graphene oxide supported Cu2O nanocubes as high active catalyst for CO2 electroreduction to C2H4. Journal of Alloys and Compounds, 2019, 785, 7-12.	5.5	63
80	Carbon Dots Decorated Hierarchical NiCo <sub>2</sub> S <sub>4</sub> /Ni <sub>3</sub> S <sub>2</sub> Composite for Efficient Water Splitting. ACS Sustainable Chemistry and Engineering, 2019, 7, 2610-2618.	6.7	49
81	Structural Modulation of Co Catalyzed Carbon Nanotubes with Cu–Co Bimetal Active Center to Inspire Oxygen Reduction Reaction. ACS Applied Materials & Interfaces, 2019, 11, 3937-3945.	8.0	51
82	3D self-assembly synthesis of hierarchical porous carbon from petroleum asphalt for supercapacitors. Carbon, 2018, 134, 345-353.	10.3	103
83	A Tunable Molten-Salt Route for Scalable Synthesis of Ultrathin Amorphous Carbon Nanosheets as High-Performance Anode Materials for Lithium-Ion Batteries. ACS Applied Materials & Interfaces, 2018, 10, 5577-5585.	8.0	84
84	Metal–Organic Frameworks Mediated Synthesis of One-Dimensional Molybdenum-Based/Carbon Composites for Enhanced Lithium Storage. ACS Nano, 2018, 12, 1990-2000.	14.6	221
85	Highly Dispersed Mo <sub>2</sub> C Anchored on N,Pâ€Codoped Graphene as Efficient Electrocatalyst for Hydrogen Evolution Reaction. ChemCatChem, 2018, 10, 2300-2304.	3.7	22
86	Multiaspect insight into synergetic modification of carbon nitride with halide salt and water vapor. Applied Catalysis B: Environmental, 2018, 229, 204-210.	20.2	18
87	Intercalating petroleum asphalt into electrospun ZnO/Carbon nanofibers as enhanced free-standing anode for lithium-ion batteries. Journal of Alloys and Compounds, 2018, 737, 330-336.	5.5	35
88	Iron carbide encapsulated by porous carbon nitride as bifunctional electrocatalysts for oxygen reduction and evolution reactions. Applied Surface Science, 2018, 439, 439-446.	6.1	34
89	Novel in-situ redox synthesis of Fe3O4/rGO composites with superior electrochemical performance for lithium-ion batteries. Electrochimica Acta, 2018, 262, 233-240.	5.2	55
90	Functionalizing carbon nitride with heavy atom-free spin converters for enhanced 1O2 generation. Journal of Catalysis, 2018, 361, 222-229.	6.2	26

#	Article	IF	CITATIONS
91	Heteromorphic NiCo <sub>2</sub> S <sub>4</sub> /Ni <sub>3</sub> S <sub>2</sub> /Ni Foam as a Self-Standing Electrode for Hydrogen Evolution Reaction in Alkaline Solution. ACS Applied Materials & Interfaces, 2018, 10, 10890-10897.	8.0	147
92	Fe-N-doped porous carbon from petroleum asphalt for highly efficient oxygen reduction reaction. Carbon, 2018, 126, 1-8.	10.3	64
93	MnS decorated N/S codoped 3D graphene which used as cathode of the lithium-sulfur battery. Applied Surface Science, 2018, 433, 10-15.	6.1	42
94	Graphene structure boosts electron transfer of dual-metal doped carbon dots in photooxidation. Carbon, 2018, 126, 128-134.	10.3	53
95	Template-free synthesis of coral-like nitrogen-doped carbon dots/Ni3S2/Ni foam composites as highly efficient electrodes for water splitting. Carbon, 2018, 129, 335-341.	10.3	55
96	Synergies between Unsaturated Zn/Cu Doping Sites in Carbon Dots Provide New Pathways for Photocatalytic Oxidation. ACS Catalysis, 2018, 8, 747-753.	11.2	53
97	Bimetal Prussian Blue as a Continuously Variable Platform for Investigating the Composition–Activity Relationship of Phosphides-Based Electrocatalysts for Water Oxidation. ACS Applied Materials & Interfaces, 2018, 10, 35904-35910.	8.0	28
98	An amorphous tin-based nanohybrid for ultra-stable sodium storage. Journal of Materials Chemistry A, 2018, 6, 18920-18927.	10.3	22
99	Lamellar Metal Organic Framework-Derived Fe–N–C Non-Noble Electrocatalysts with Bimodal Porosity for Efficient Oxygen Reduction. ACS Applied Materials & Interfaces, 2017, 9, 5272-5278.	8.0	95
100	Moldable clay-like unit for synthesis of highly elastic polydimethylsiloxane sponge with nanofiller modification. RSC Advances, 2017, 7, 10479-10486.	3.6	16
101	Controllable growth of MnO <sub>x</sub> dual-nanocrystals on N-doped graphene as lithium-ion battery anode. RSC Advances, 2017, 7, 6396-6402.	3.6	9
102	Cation modulating electrocatalyst derived from bimetallic metal–organic frameworks for overall water splitting. Journal of Materials Chemistry A, 2017, 5, 6170-6177.	10.3	58
103	Supramolecular polymerization-assisted synthesis of nitrogen and sulfur dual-doped porous graphene networks from petroleum coke as efficient metal-free electrocatalysts for the oxygen reduction reaction. Journal of Materials Chemistry A, 2017, 5, 11331-11339.	10.3	54
104	Electrospinning ZnO/carbon nanofiber as binder-free and self-supported anode for Li-ion batteries. Journal of Alloys and Compounds, 2017, 722, 716-720.	5.5	44
105	Combination of Nitrogen-Doped Graphene with MoS2 Nanoclusters for Improved Li-S Battery Cathode: Synthetic Effect between 2D Components. Electrochimica Acta, 2017, 252, 200-207.	5.2	52
106	Enhancing Selective Photooxidation through Co–Nx-doped Carbon Materials as Singlet Oxygen Photosensitizers. ACS Catalysis, 2017, 7, 7267-7273.	11.2	111
107	Synergistic Effects between Doped Nitrogen and Phosphorus in Metal-Free Cathode for Zinc-Air Battery from Covalent Organic Frameworks Coated CNT. ACS Applied Materials & Interfaces, 2017, 9, 44519-44528.	8.0	65
108	Substrate-Assisted in Situ Confinement Pyrolysis of Zeolitic Imidazolate Frameworks to Nitrogen-Doped Hierarchical Porous Carbon Nanoframes with Superior Lithium Storage. ACS Applied Materials & Interfaces, 2017, 9, 42845-42855.	8.0	13

#	Article	IF	CITATIONS
109	Synergistically enhanced activity of nitrogen-doped carbon dots/graphene composites for oxygen reduction reaction. Applied Surface Science, 2017, 423, 909-916.	6.1	44
110	Preparation of carbon nanosheets from petroleum asphalt via recyclable molten-salt method for superior lithium and sodium storage. Carbon, 2017, 122, 344-351.	10.3	99
111	A green and template recyclable approach to prepare Fe3O4/porous carbon from petroleum asphalt for lithium-ion batteries. Journal of Alloys and Compounds, 2017, 695, 2612-2618.	5.5	49
112	Preparation of polystyrene@CdS core-shell nanocomposite materials with different cadmium sources for photocatalysis. Inorganic and Nano-Metal Chemistry, 2017, 47, 737-743.	1.6	0
113	Hydrotalcite-like Ni(OH) <sub>2</sub> Nanosheets in Situ Grown on Nickel Foam for Overall Water Splitting. ACS Applied Materials & Interfaces, 2016, 8, 33601-33607.	8.0	204
114	Remedying Defects in Carbon Nitride To Improve both Photooxidation and H <sub>2</sub> Generation Efficiencies. ACS Catalysis, 2016, 6, 3365-3371.	11.2	148
115	A layered-template-nanospace-confinement strategy for production of corrugated graphene nanosheets from petroleum pitch for supercapacitors. Chemical Engineering Journal, 2016, 297, 121-127.	12.7	168
116	Advanced visible-light driven photocatalyst with enhanced charge separation fabricated by facile deposition of Ag 3 PO 4 nanoparticles on graphene-like h -BN nanosheets. Journal of Molecular Catalysis A, 2016, 424, 135-144.	4.8	34
117	Soy flour-derived carbon dots: facile preparation, fluorescence enhancement, and sensitive Fe3+ detection. Journal of Nanoparticle Research, 2016, 18, 1.	1.9	27
118	Influence of two different template removal methods on the micromorphology, crystal structure, and photocatalytic activity of hollow CdS nanospheres. Journal of Nanoparticle Research, 2016, 18, 1.	1.9	7
119	Shell-like hierarchical porous carbons for high-rate performance supercapacitors. Microporous and Mesoporous Materials, 2016, 236, 134-140.	4.4	50
120	Firmly combination of CoMnO x nanocrystals supported on N-doped CNT for lithium-ion batteries. Chemical Engineering Journal, 2016, 306, 336-343.	12.7	26
121	Engineering surface structure of petroleum-coke-derived carbon dots to enhance electron transfer for photooxidation. Journal of Catalysis, 2016, 344, 236-241.	6.2	34
122	Green fabrication of magnetic recoverable graphene/MnFe <sub>2</sub> O <sub>4</sub> hybrids for efficient decomposition of methylene blue and the Mn/FeÂredox synergetic mechanism. RSC Advances, 2016, 6, 104549-104555.	3.6	50
123	Utilization of spent aluminum for p-arsanilic acid degradation and arsenic immobilization mediated by Fe(II) under aerobic condition. Chemical Engineering Journal, 2016, 297, 45-54.	12.7	24
124	In situ growth of polyphosphazene nanoparticles on graphene sheets as a highly stable nanocomposite for metal-free lithium anodes. RSC Advances, 2016, 6, 62005-62010.	3.6	7
125	Synthesis of ultrathin hollow carbon shell from petroleum asphalt for high-performance anode material in lithium-ion batteries. Chemical Engineering Journal, 2016, 286, 632-639.	12.7	86
126	Self-assembly of disordered hard carbon/graphene hybrid for sodium-ion batteries. Journal of Power Sources, 2016, 305, 156-160.	7.8	61

#	Article	IF	CITATIONS
127	Synthesis of three dimensional extended conjugated polyimide and application as sodium-ion battery anode. Chemical Engineering Journal, 2016, 287, 516-522.	12.7	90
128	Engineering monomer structure of carbon nitride for the effective and mild photooxidation reaction. Carbon, 2016, 100, 450-455.	10.3	65
129	The roles of polycarboxylates in Cr(VI)/sulfite reaction system: Involvement of reactive oxygen species and intramolecular electron transfer. Journal of Hazardous Materials, 2016, 304, 457-466.	12.4	49
130	Active and regioselective rhodium catalyst supported on reduced graphene oxide for 1-hexene hydroformylation. Catalysis Science and Technology, 2016, 6, 1162-1172.	4.1	45
131	SO3H-modified petroleum coke derived porous carbon as an efficient solid acid catalyst for esterification of oleic acid. Journal of Porous Materials, 2016, 23, 263-271.	2.6	26
132	Combination of uniform SnO2 nanocrystals with nitrogen doped graphene for high-performance lithium-ion batteries anode. Chemical Engineering Journal, 2016, 283, 1435-1442.	12.7	88
133	Intramolecular Charge Transferâ€Enhanced BODIPY Photosensitizer in Photoinduced Electron Transfer and Its Application to Photoxidation under Mild Condition. Chinese Journal of Chemistry, 2015, 33, 1251-1258.	4.9	7
134	Cu–N Dopants Boost Electron Transfer and Photooxidation Reactions of Carbon Dots. Angewandte Chemie - International Edition, 2015, 54, 6540-6544.	13.8	244
135	Monodispersed Hollow SO <sub>3</sub> H-Functionalized Carbon/Silica as Efficient Solid Acid Catalyst for Esterification of Oleic Acid. ACS Applied Materials & Interfaces, 2015, 7, 26767-26775.	8.0	124
136	Enteromorpha based porous carbons activated by zinc chloride for supercapacitors with high capacity retention. RSC Advances, 2015, 5, 16575-16581.	3.6	47
137	High-Efficiency Simultaneous Oxidation of Organoarsenic and Immobilization of Arsenic in Fenton Enhanced Plasma System. Industrial & Engineering Chemistry Research, 2015, 54, 8277-8286.	3.7	36
138	Synthesis of nanocomposites with carbon–SnO2 dual-shells on TiO2 nanotubes and their application in lithium ion batteries. Journal of Materials Chemistry A, 2015, 3, 16057-16063.	10.3	53
139	Photocatalytic H2 evolution from NADH with carbon quantum dots/Pt and 2-phenyl-4-(1-naphthyl)quinolinium ion. Journal of Photochemistry and Photobiology B: Biology, 2015, 152, 63-70.	3.8	28
140	Synergetic effect of C*N^N/C^N^N coordination and the arylacetylide ligands on the photophysical properties of cyclometalated platinum complexes. Journal of Materials Chemistry C, 2015, 3, 2291-2301.	5.5	37
141	Facile synthesis of ZnO/mesoporous carbon nanocomposites as high-performance anode for lithium-ion battery. Chemical Engineering Journal, 2015, 271, 173-179.	12.7	81
142	Synergetic Transformations of Multiple Pollutants Driven by Cr(VI)–Sulfite Reactions. Environmental Science & Technology, 2015, 49, 12363-12371.	10.0	163
143	Dense 3D Graphene Macroforms with Nanotuned Pore Sizes for High Performance Supercapacitor Electrodes. Journal of Physical Chemistry C, 2015, 119, 24373-24380.	3.1	32
144	Three-dimensional ZnMn2O4/porous carbon framework from petroleum asphalt for high performance lithium-ion battery. Electrochimica Acta, 2015, 180, 164-172.	5.2	73

#	Article	IF	CITATIONS
145	A green approach towards simultaneous remediations of chromium(VI) and arsenic(III) in aqueous solution. Chemical Engineering Journal, 2015, 262, 1144-1151.	12.7	58
146	Improvements of heat resistance and adhesive property of condensed poly-nuclear aromatic resin via epoxy resin modification. Petroleum Science, 2014, 11, 578-583.	4.9	7
147	Properties of a three-dimensionally ordered macro-mesoporous carbon-doped TiO2 composite catalyst. Functional Materials Letters, 2014, 07, 1350068.	1.2	9
148	Synthesis mechanism, enhanced visible-light-photocatalytic properties, and photogenerated hydroxyl radicals of PS@CdS core–shell nanohybrids. Journal of Nanoparticle Research, 2014, 16, 1.	1.9	14
149	Broadband Absorbing Polyporphyrin Membrane as Singlet Oxygen Photosensitizer for Photoâ€oxidation. Macromolecular Chemistry and Physics, 2014, 215, 280-285.	2.2	8
150	Synthesis of starch-derived mesoporous carbon for electric double layer capacitor. Chemical Engineering Journal, 2014, 245, 166-172.	12.7	99
151	Graphene enhanced carbon-coated tin dioxide nanoparticles for lithium-ion secondary batteries. Journal of Materials Chemistry A, 2014, 2, 7471-7477.	10.3	65
152	Pt Nanocatalysts Supported on Reduced Graphene Oxide for Selective Conversion of Cellulose or Cellobiose to Sorbitol. ChemSusChem, 2014, 7, 1398-1406.	6.8	89
153	Preparation of functionalized water-soluble photoluminescent carbon quantum dots from petroleum coke. Carbon, 2014, 78, 480-489.	10.3	210
154	BODIPY-based photosensitizers with intense visible light harvesting ability and high <sup>1</sup> O <sub>2</sub> quantum yield in aqueous solution. RSC Advances, 2014, 4, 51349-51352.	3.6	24
155	Microwave-assisted synthesis of Ru/mesoporous carbon composites for supercapacitors. Materials Letters, 2014, 115, 96-99.	2.6	24
156	Pt Nanoparticles Loaded on Reduced Graphene Oxide as an Effective Catalyst for the Direct Oxidation of 5-Hydroxymethylfurfural (HMF) to Produce 2,5-Furandicarboxylic Acid (FDCA) under Mild Conditions. Bulletin of the Chemical Society of Japan, 2014, 87, 1124-1129.	3.2	32
157	Synthesis of condensed polynuclear aromatic resin from furfural extract oil of reduced-pressure route II. Petroleum Science, 2013, 10, 584-588.	4.9	4
158	Facile preparation of mesoporous carbons for supercapacitors by one-step microwave-assisted ZnCl2 activation. Materials Letters, 2013, 94, 158-160.	2.6	43
159	The preparation, load and photocatalytic performance of N-doped and CdS-coupled TiO2. RSC Advances, 2013, 3, 9483.	3.6	20
160	Confinement Effect of Carbon Nanotubes: Copper Nanoparticles Filled Carbon Nanotubes for Hydrogenation of Methyl Acetate. ACS Catalysis, 2012, 2, 1958-1966.	11.2	138
161	Hydrothermal co-doping of boron and phosphorus into porous carbons prepared from petroleum coke to improve oxidation resistance. Materials Letters, 2012, 82, 124-126.	2.6	11
162	Preparation of porous carbons from petroleum coke by different activation methods. Fuel, 2005, 84, 1992-1997.	6.4	79

#	Article	IF	CITATIONS
163	Cesium Salts as Mild Chemical Scissors To Trim Carbon Nitride for Photocatalytic H <sub>2</sub> Evolution. ACS Sustainable Chemistry and Engineering, 0, , .	6.7	2